Influence of Tropospheric Water Vapor Corrections on Geosat Altimetry in the North Atlantic Ocean

NORBERT DIDDEN AND DETLEF STAMMER*

Institut für Meereskunde an der Universität Kiel, Kiel, Germany

(Manuscript received 12 July 1993, in final form 23 December 1993)

ABSTRACT

Geosat sea surface height (SSH) data in the tropical and midlatitude North Atlantic are analyzed with and without water vapor (WV) corrections to study the WV influence on along-track SSH anomaly profiles, mesoscale SSH variability, wavenumber spectra, and objectively mapped fields of SSH anomaly. Three different WV datasets were used, one from the Fleet Numerical Oceanographic Center (FNOC) model and two from the Special Sensor Microwave/Imager (SSM/I) based on different WV retrieval algorithms. These WV datasets show significant differences, in particular in the tropics. However, the method for deriving SSH anomalies from altimeter height data filters out much of the WV corrections. The residual WV effect on SSH anomaly is shown to be most significant in the seasonally migrating intertropical convergence zone of the tropical Atlantic: there the SSM/I corrections reduce the along-track mesoscale SSH variability by typically 1–1.5 cm. On seasonal timescales the maximum WV effect in this region is characterized by a 2–3-cm rms difference between SSH anomaly with and without SSM/I WV corrections, whereas FNOC corrections have almost no effect. Inferred seasonal velocity variations in the North Equatorial Countercurrent core (4°–6°N) in the region of maximum WV influence (30°–40°W) are reduced by about 20% and 30%, depending on whether SSM/I corrections by Emery or Wentz are used.

1. Introduction

During the last decade a rapid development in satellite altimetry and its use for ocean studies has taken place. The precise observation of sea surface height (SSH) from space requires the correction of various environmental effects on the altimetric pulse travel time. Among these the most critical term is due to tropospheric water vapor (WV) content. Since the spatial scales of this correction are comparable to ocean phenomena and its amplitude ranges from a few centimeters at high latitudes to 40 cm near the equator, its signal resembles oceanic sea surface height variability in many places of the world oceans.

Until now, most altimetric studies were based on data of the recent Geosat altimeter mission. In contrast to the early Seasat and the ongoing *ERS-1* and Topex–Poseidon altimeter missions, there was no microwave radiometer on board Geosat and the atmospheric WV content was not measured simultaneously with the altimetry. Therefore the initial release of Geosat geophysical data records (GDR) (Cheney et al. 1987) contains WV corrections that are derived from other data sources, such as the Fleet Numerical Oceanographic Center (FNOC) meteorological model that is known to not adequately resolve synoptic atmospheric structures and to systematically underestimate the WV in the tropics (Emery et al. 1990). However, Geosat altimeter SSH data based on FNOC WV corrections have successfully been used for a wide range of oceanographic studies: for mesoscale eddy detection and tracking (e.g., Willebrand et al. 1990; Gordon and Haxby 1990; Stammer et al. 1991; Didden and Schott 1993), for studies of space and timescales of the mesoscale eddy field (LeTraon et al. 1990; Stammer and Böning 1992) as well as on seasonal and interannual timescales of the SSH field and the inferred geostrophic current variability (e.g., Arnault et al. 1992; Didden and Schott 1992), and for data assimilation (e.g., White et al. 1990; Moore 1991; Holland et al. 1992). Since precise WV data were lacking in all studies based on the original GDRs, it was not possible to give more than a rough estimate of the effect of WV errors on ocean results.

The recent WV corrections derived from the Special Sensor Microwave/Imager (SSM/I) flown on a DMSP (Defense Meteorological Satellite Program) satellite are generally considered to be more accurate (Emery et al. 1990; Wentz 1990). For a full spatial coverage, how-

* Current affiliation: Massachusetts Institute of Technology, Cambridge, Massachusetts.

Corresponding author address: Dr. Norbert Didden, Institut für Meereskunde an der Universität Kiel, Regionale Ozeanographie, Düsternbrooker Weg 20, D-24105 Kiel, Germany.

ever, the SSM/I WV data have to be averaged over 1° × 1° boxes in space and over at least a 4-day period. Therefore, in regions of considerable WV variability on timescales of less than 2 days (Minster et al. 1992), the data are not synoptic and thus the time difference of up to 4 days between Geosat and SSM/I measurements may introduce significant correction errors.

By comparison with the more reliable WV corrections from SSM/I data we are now able to quantitatively estimate the SSH error made by using FNOC WV corrections. Previous studies on the error of WV corrections focused on differences between different WV datasets (Zimbelman and Busalacchi 1990; Emery et al. 1990). However, since in most ocean studies only the time variations of altimetric SSH are analyzed (i.e., SSH residuals from a temporal mean), the degrading influence of WV correction errors is considerably reduced due to the filtering effects of several processing steps involved in the Geosat data analysis: the collinear analysis, the orbit error correction, and the space–time objective mapping of the along-track SSH data. Some aspects of this filtering effect on WV corrections have been discussed already by Jourdan et al. (1990) for mesoscale signals in a small region of the northeast Atlantic and by Cheney et al. (1991) for seasonal SSH variations in the tropical Pacific.

The aim of the present paper is to provide a more general indication of the uncertainties of final altimeter products when applying WV corrections from different datasets. We therefore evaluate the reduction of the WV correction due to the various SSH processing steps and the remaining impact of the different WV corrections on the final SSH anomaly estimates. The WV data used here are from (i) the FNOC model and from (ii) SSM/I microwave radiometer measurements. Two sets of SSM/I corrections are used based on different algorithms for estimating WV from brightness temperatures, one of Emery et al. (1990) and one of Wentz (1990), respectively. Comparison of the results from the latter two datasets are suitable to indicate the uncertainty in the estimate of the WV correction due to the retrieval algorithms.

In the following, we study the differences between these WV datasets (section 3) as well as the WV influence on the statistics of along-track mesoscale SSH anomalies (section 4). The regional dependence of this influence on the along-track wavenumber characteristics of the WV data and of the oceanic SSH signal are discussed in section 5. The WV influence on synoptic maps of SSH anomalies is studied in section 6. In particular, it is shown how the WV corrections influence the seasonal variations of SSH and geostrophic currents in the tropical Atlantic.

2. Database and method

a. Geosat data

Since SSM/I WV measurements are not available before July 1987, only the 1-yr period from July 1987 to June 1988 during the Geosat Exact Repeat Mission (ERM) was chosen for this study. Since the intention of this paper is to estimate uncertainties of previous studies, our analysis is based on the original GDRs containing the Navy Astronautics Group (NAG) GEM-10 orbits. After editing the GDRs for spurious SSH data (for details see Willebrand et al. 1990; Didden and Schott 1992), the usual corrections for ionospheric path delay, dry troposphere, solid earth, and ocean tides were applied. We further corrected for atmospheric pressure loading and for sea-state bias using 2% of the significant wave height. Because of uncertainties of the tide corrections in shallow water, data in continental shelf regions were excluded.

With respect to tropospheric WV corrections four different datasets were produced: (i) without WV corrections, (ii) with FNOC WV corrections (FNOC) and with two different SSM/I WV corrections derived by (iii) Emery (SSM/I-Em) and by (iv) Wentz (SSM/I-We). These four datasets were interpolated onto a fixed 6.8-km along-track grid and the collinear method was applied separately in the two latitude bands 10°S–30°N and 20°–60°N: for each track a 1-yr mean sea level over 22 repeated Geosat passes (sampled every 17.05 days) was subtracted from each individual pass. For the mean sea level estimation a reference pass method (see Didden and Schott 1992, henceforth called DS92) was used to avoid a bias due to the 4-m rms orbit error at data gaps in temporal sampling. The orbit error was removed by subtracting quadratic polynomials fitted by least-squares methods over 40° arcs (typically 5000 km). For incomplete arcs shorter than 1000 km only bias and trend were subtracted.

The SSH anomaly profiles (residuals relative to the 1-yr mean) were subsequently filtered over 20 km in the midlatitude band 20°–60°N and over 70 km in the tropical band (10°S–30°N) and then subsampled at 20-km intervals. From these along-track SSH anomalies, quasisynoptic maps were estimated by space–time interpolation onto a regular grid, using an objective analysis method that is specifically suited for large altimeter datasets (DeMey and Menard 1989). Correlation scales of 100 km, 15 days were used in the midlatitude band and 300 km, 30 days in the tropical region.

b. Water vapor data

To explain differences in the applied WV datasets, we start with a brief summary of the basic assumptions inherent in methods for retrieving atmospheric water vapor.

The tropospheric WV causes a radar pulse path delay that results in a height correction h_{wv} (m) given by (see Chelton 1988)

$$h_{wv} = 0.373 \int \frac{e(z)}{T(z)} dz. \qquad (1)$$

Here $e(z)$ and $T(z)$ describe the vertical distributions of water vapor partial pressure (hPa), and of temperature (K), respectively. Assuming a standard atmosphere characterized by a WV pressure distribution

$$\frac{e(z)}{e_0} = \left[\frac{T(z)}{T_0}\right]^{\alpha}, \tag{2}$$

with an exponent α being constant for constant vertical pressure gradient, the height correction (1) can be related to the surface values of WV pressure e_0 and temperature T_0 by (Saastamoinen 1972)

$$h_{wv} = 2277\left(\frac{1255}{T_0} + 0.05\right)e_0 . \tag{3}$$

Another approach is to approximate (1) by the relation (Tapley et al. 1982)

$$h_{wv} = 0.0631W, \tag{4}$$

where W (g cm^{-2}) represents the vertically integrated (total column) atmospheric WV content.

The FNOC WV corrections provided with the Geosat GDRs are based on (3) and on the surface values e_0, T_0 of the FNOC meteorological model. The model WV corrections are provided every 12 h on a global grid of 2.5° resolution and are interpolated in space and time onto the Geosat 1-Hz along-track foot points. Potential errors in the estimate of FNOC WV corrections are associated with (i) errors of the model fields, (ii) insufficient spatial resolution of 2.5° to adequately resolve smaller-scale atmospheric structures like fronts with strong cross-front WV gradients, and (iii) the neglect of deviations from the standard atmospheric profile of (2). Deviations from the standard profile are particularly large in the tropics, where the relative amount of WV is increased at high altitude and the WV correction based on surface WV vapor pressure e_0 [Eq. (3)] is underestimated in the FNOC model.

The SSM/I WV correction data on the other hand are based on relation (4). The total WV content W is derived from brightness temperatures of different SSM/I channels. Emery et al. (1990) derived the SSM/I-Em WV data using a linear combination of brightness temperatures from two SSM/I channels with a claimed accuracy of 0.16 g cm^{-2} (or 1.0 cm). The dataset consists of global 1° × 1° maps of 7-day averages in 1987 and 4-day averages in 1988. For interpolating these data onto Geosat passes we used an interpolation quadratic in time and bilinear in space. The second SSM/I WV dataset (SSM/I-We), computed by Wentz (1983, 1990) from brightness temperatures using a nonlinear algorithm with an accuracy of 0.3 g cm^{-2} (or 1.9 cm), was kindly provided by the NASA (National Aeronautics and Space Administration) Ocean Data System (NODS) at the Jet Propulsion Laboratory in California. It consists of WV corrections interpolated from global 4-day averages in 1° × 1° squares onto Geosat tracks at 10-s intervals. The 4-day averaging is required to get complete global coverage. Each individual grid point consists of data from 1 to 8 SSM/I swaths. These WV data, due to insufficient sampling in time, do not resolve small-scale atmospheric structures (with timescales of a day) like moving frontal systems associated with strong cross-front WV gradients. From the comparison of 4-day averages from Wentz with estimates derived from space–time objective analysis, Minster et al. (1992) reported WV differences typically less than 6 cm (for 90% of the global dataset), but with maximum values up to 12 cm.

3. Along-track WV corrections

The 1-yr mean WV corrections along a Geosat track crossing the Atlantic Ocean (Fig. 1a) display the characteristic large-scale meridional distribution of atmospheric WV with low values at high latitudes and a maximum in the tropics, which is associated with the mean meridional position of the intertropical convergence zone (ITCZ) at about 5°N. Large differences in the mean WV correction between FNOC and SSM/I data (up to 10 cm) are particularly obvious in the tropics, where the 1-yr rms variability for SSM/I corrections (Fig. 1b) is also considerably higher than for FNOC corrections.

While the increased WV variability at midlatitudes is associated with fast-moving weather systems, the pronounced double peak of the SSM/I WV variability in the tropics with maxima near the equator and at 10°N is related to the turning latitudes of the annual meridional migration of the ITCZ. Since the variability

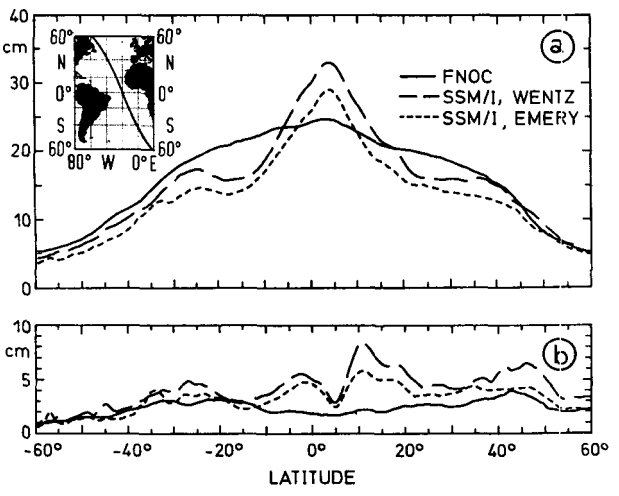

FIG. 1. Intercomparison of water vapor (WV) corrections from FNOC, SSM/I-We, and SSM/I-Em datasets along the Geosat track shown in the inset: 1-yr statistics for repeat cycles 15–36. (a) Mean and (b) standard deviation of WV correction.

structure in the tropics is missing in the FNOC corrections, the vertically integrated WV content in the ITCZ is obviously not well represented by the surface humidity in the FNOC model. Note that the mean and variability of the SSM/I-Em corrections are generally a few cm lower than for SSM/I-We corrections. This is most likely due to the different algorithms used. In addition, the variability of the Emery data may be lower partly due to 7-day averaging for the 1987 period (section 2b).

The WV corrections are added to the along-track SSH signals before SSH anomalies are estimated using the linear operations of the collinear analysis, that is, subtraction of both the 1-yr temporal mean and the orbit error estimated from linear least-squares fit. Thus the filtering effects of these procedures apply to the WV corrections and their associated errors as well and it is not the absolute WV correction and WV error that matters, but their residuals after applying the analysis procedures. Of course this is true for all applied environmental height corrections. The influence of WV corrections on the final SSH anomalies can therefore be estimated by applying the same procedures to the WV corrections only. This results in WV anomalies, which are identical to the difference between SSH anomalies computed with and without WV corrections.

The effects of the processing steps on the WV contribution to SSH anomalies are illustrated in Fig. 2 using a single along-track profile of repeat cycle 20 of the same track as in Fig. 1. The WV corrections (Fig. 2a) are first reduced by subtracting the 1-yr mean profile in the collinear analysis (Fig. 2b). This step reduces the differences between different WV corrections and the large-scale residual WV distributions become very similar north of 15°N on scales exceeding 5°. Removal of the orbit error modeled by quadratic polynomials over 40° arcs (4800 km along track) results in WV anomalies as shown in Fig. 2c. It should be noted that the orbit error correction filters out large-scale variability of both WV corrections and SSH. For the orbit error model chosen here the orbit error of wavenumber one per revolution is well removed (Tai 1989). On the other hand, it should not seriously degrade the SSH variability for studies of either mesoscale eddies or seasonal fluctuations in the tropics associated with zonal current bands of small meridional scales. Similar to the mean profiles the individual realizations show a systematic difference between FNOC and SSM/I data, in particular in the tropics. Differences between SSM/I-Em and SSM/I-We datasets are again partly due to the different averaging periods.

The 1-yr rms variability of WV anomaly (Fig. 2d) clearly shows the difference between FNOC and SSM/I WV contribution to SSH anomaly in the 5°S–15°N latitude band: the double peak of SSM/I data is still present, although with reduced amplitude. Outside the tropical latitude band the FNOC and SSM/I-Em

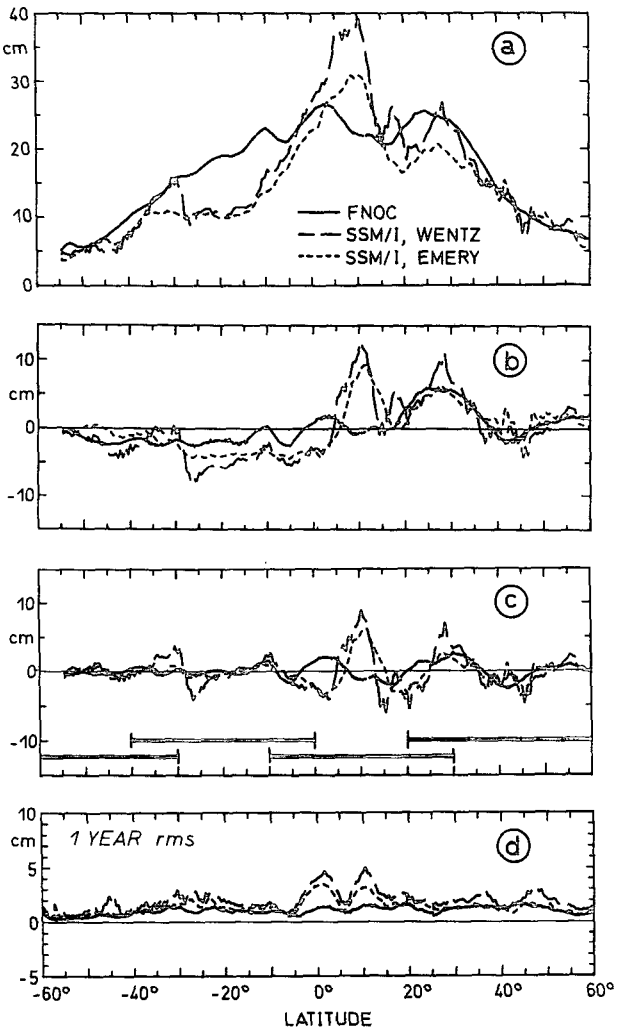

FIG. 2. Successive steps of WV anomaly computation (equivalent to SSH anomaly computation by collinear analysis) for the same track as in Fig. 1. (a) FNOC, SSM/I-We, and SSM/I-Em WV corrections of cycle 20 in October 1987. (b) Same after subtracting 1-yr mean. (c) The WV anomaly after subtraction of quadratic polynomial fitted over 40° arcs (heavy bars) for "orbit error correction." (d) The rms variability of WV anomaly over 1 yr.

variability levels are similar, but lower than SSM/I-We. The overall filter effect of the analysis procedure is characterized by the change of the variability level of WV correction (Fig. 1b) against WV correction anomaly (Fig. 2d): the mean variability in the 60°S–60°N range is reduced from 2.4, 3.2, and 4.1 cm to 1.1, 1.7, and 2.0 cm for the FNOC, SSM/I-Em, and SSM/I-We corrections, respectively, that is, by about 50%.

4. Along-track SSH anomaly

The sensitivity of SSH estimates to WV corrections and to associated WV errors depends on the magnitude

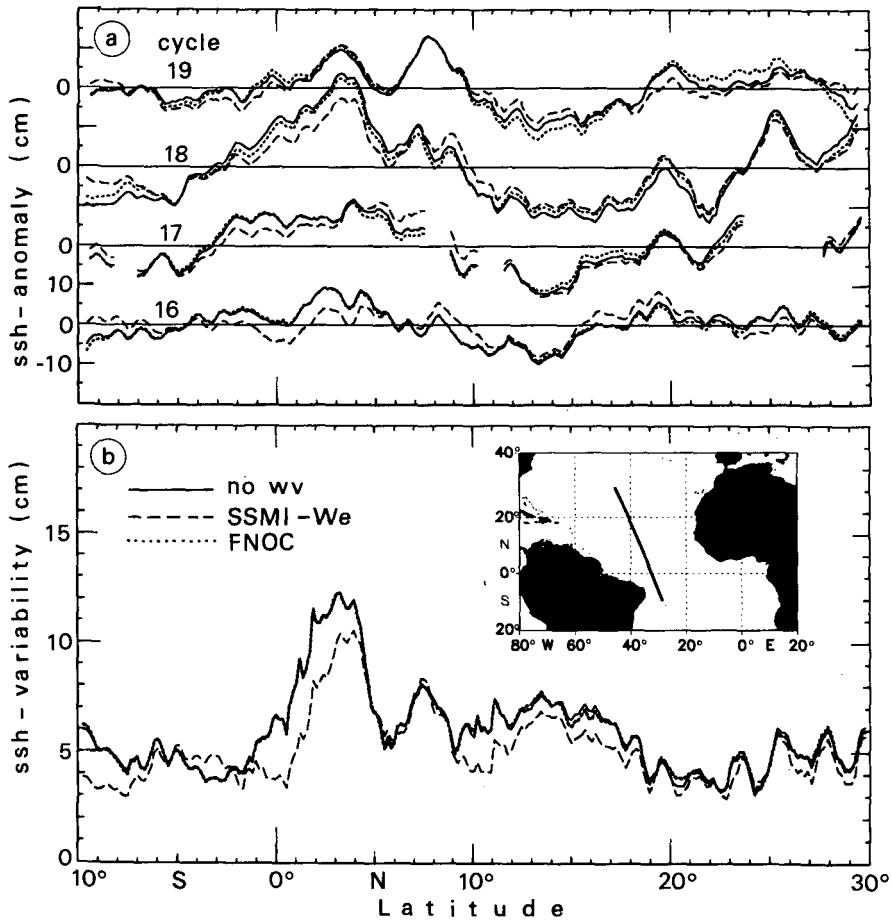

FIG. 3. SSH anomaly along a Geosat track [see inset in (b)] crossing the tropics in the region of maximum WV variability: (a) examples for cycles 16–19 of SSH anomaly applying no WV correction (solid), FNOC correction (dotted), and SSM/I-We correction (dashed). (b) One-year SSH variability with the different WV corrections.

of WV anomaly relative to SSH anomaly. In the next step we compare SSH anomalies derived without applying WV correction with those using the different WV datasets.

In Fig. 3, some SSH anomaly profiles in the tropical band 10°S–30°N are displayed along a track crossing the equator at 34°W. This track was chosen because it crosses the region of high SSH variability in the western tropical Atlantic centered near 5°N, 35°W as well as the region of maximum WV variability. The along-track variability statistics are given in Table 1. The dominant spatial scales of the SSH differences with and without WV corrections are 500 km and larger for both FNOC and SSM/I-We corrections (Fig. 3a), and the overall spatial structure of SSH variability is almost unchanged (Fig. 3b). When using FNOC WV corrections the maximum change of SSH anomaly is about 2 cm, resulting in a change of SSH variability by less

TABLE 1. Water vapor and SSH variability for the 10°S–30°N region over 1 yr (22 cycles) for the Geosat track of Fig. 3.

WV correction	Mean WV (cm)	σ (WV) (cm)	σ (WV anomaly) (cm)	σ (SSH anomaly) (cm)	Relative change due to WV correction
No WV correction	—	—	—	6.2	—
FNOC	22.8	2.5	1.0	6.2	$< -1\%$
SSM/I-Em	21.7	6.0	1.9	5.7	-7%
SSM/I-We	25.0	6.8	2.7	5.4	-14%

than 1% (Fig. 3b and Table 1). The SSH fluctuations are significantly reduced when WV corrections of SSM/I-We are used, in particular in the 1°S–4°N and 9°–18°N latitude bands: there the reduction of 1-yr variability is 2–3 cm (Fig. 3b). Over the 10°S–30°N range the SSH variability is changed by 14% (Table 1). The corresponding reduction of SSH variability is considerably smaller (7%) when SSM/I-Em WV corrections are applied. The reduction of SSH variability when applying SSM/I-We WV correction rather than FNOC WV correction indicates that WV variability contributes to SSH variability along profiles corrected with FNOC WV content.

The geographical distribution of WV influence is shown in Fig. 4: the SSH variability map at 2° square resolution is estimated from 1 yr of along-track uncorrected SSH data (Fig. 4a). When FNOC corrections are applied, the SSH variability changes by less than 0.2 cm (not shown). The change in variability when SSM/I-We corrections are applied is shown in Fig. 4b. In the high-variability region of the western North Atlantic as well as in the low-variability region of the eastern and subtropical North Atlantic north of about 20°N the SSH variability changes by less than 0.5 cm when SSM/I-We WV corrections are applied. The band of high SSH variability (>6 cm) in the western tropical Atlantic is mainly due to the equatorial circulation system, in particular the seasonal cycle of the North Equatorial Countercurrent (NECC) centered at 5°N (DS92). The maximum change of SSH variability (Fig. 4b) occurs in the zonal bands near 2°N and is less pronounced near 10°N. It is associated with the annual migration of the ITCZ with maximum variation of WV anomaly at the northernmost and southernmost seasonal positions of the ITZC, which is also seen in Fig. 2d. In these regions the SSH variability of 6–8 cm is typically reduced by 0.7–1.5 cm.

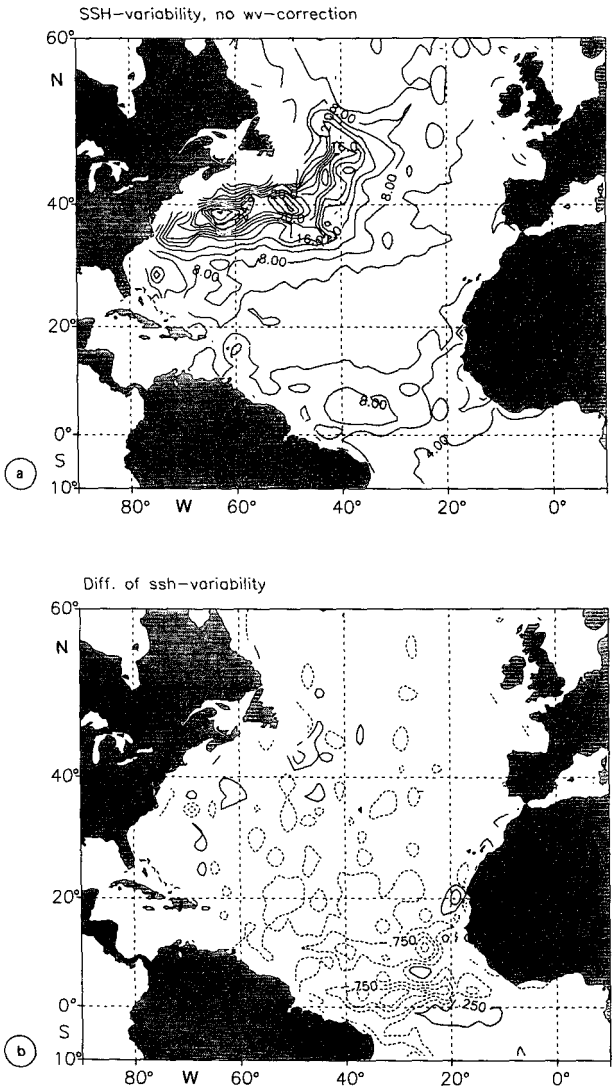

FIG. 4. Along-track SSH anomaly statistics within 2° × 2° squares for the North Atlantic. (a) SSH variability without applying WV corrections (contour interval is 2 cm). (b) Difference between SSH variabilities with and without SSM/I-We corrections (contour interval is 0.5 cm).

5. Wavenumber statistics

High-resolution along-track altimeter data have been repeatedly used to estimate the characteristics of the ocean mesoscale eddy field (Fu 1983; Fu and Zlotnicki 1989; Le Traon et al. 1990; Stammer and Böning 1992). All those studies were intended to identify possible eddy generation mechanisms from characteristics of wavenumber spectra, for example, hydrodynamic instability versus windforcing or flow interaction with topography. Yet conclusions are contradictory. The uncertainty of the SSH wavenumber spectra due to WV errors was estimated by Fu (1983) using information from the Scanning Multichannel Microwave Radiometer on Seasat. The author argues that the impact of the influence of WV error is small at wavelengths of energetic mesoscale eddies, but is likely to increase on scales exceeding 500 km. For low-energy areas this implies that at these wavelengths the spectra will be dominated by the characteristics of WV errors. However, as relevant for the discussion of uncertainties of the final altimeter results, the filter effect of the analysis procedure has not been taken into account while discussing wavenumber spectra.

Here we investigate the spatial scales on which SSH along-track wavenumber spectra are influenced by the FNOC and SSM/I WV corrections. Figure 5 shows wavenumber spectra from all Geosat tracks at low latitudes 0°–20°N (Fig. 5a) and midlatitudes 20°–40°N (Fig. 5b) in the indicated 30° longitude ranges. Spectra and autocorrelation functions are computed over 20° profiles (2400 km) after orbit error correction over 40°

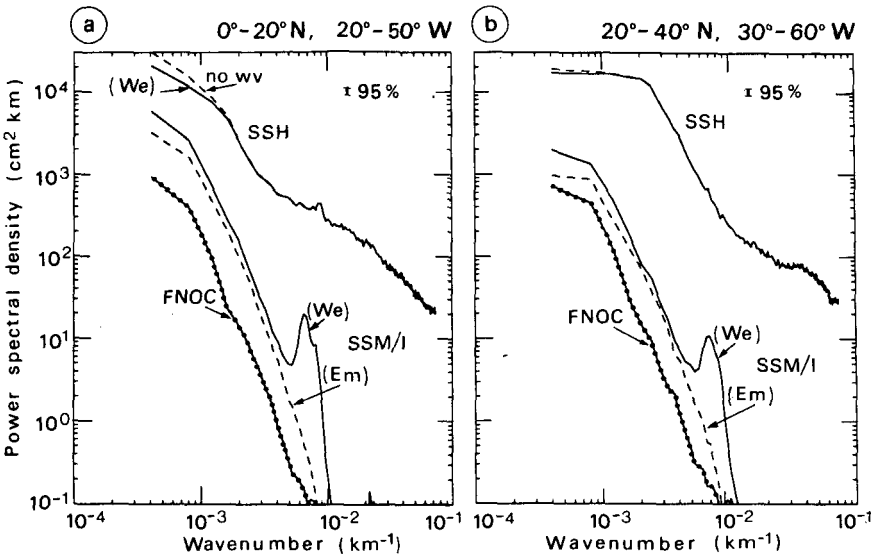

FIG. 5. Wavenumber spectra of WV correction anomaly and of SSH anomaly in (a) the western tropical and (b) the midlatitude North Atlantic. The spectra of SSH with FNOC corrections (not shown) and with no WV corrections (dashed) coincide.

arc segments, using the methodology described in Stammer and Böning (1992). Profiles shorter than 1700 km were rejected. Note, that the quadratic polynomial correction over 40° arc segments reduces the amplitude of the 20° wavelength signal (corresponding to the lowest spectral wavenumber 4×10^{-4} km^{-1}) by only 5% (Tai 1989). Thus the spectra should be realistic at all wavenumbers. For spectrum calculation a cosine taper over 10% of the record length was applied at both ends of the profiles. The tapering reduces the rms variability at all wavelengths by about 7% and leaves the spectral slope unchanged.

The WV spectra agree remarkably in shape, showing a pronounced cutoff roughly at 1000 km, the characteristic scale of atmospheric synoptic disturbances. The spectral slope toward higher wavenumber is close to a k^{-4} relation. However, the energy levels between the WV corrections show significant differences, with highest energy for the Wentz data. The slightly lower spectral energy of the Emery WV corrections is mainly attributed to the 7-day averaging as compared to 4-day averaging of the Wentz data. Note, that the high wavenumber peak of Wentz corrections is most likely a result of Wentz's interpolation method for mapping WV data onto Geosat tracks at 70 km along-track spacing, which corresponds to twice the peak wavenumber.

The spectral energy of the WV corrections is more than 1 decade lower than the energy of SSH anomaly for all wavenumbers except for SSM/I corrections in the low-latitude band at wavelengths exceeding 600 km (Fig. 5a). In this latter long-wavelength regime (wavenumber less than 1.7×10^{-3} km^{-1}), the energy of uncorrected SSH anomalies is reduced when SSM/I-We WV corrections are applied, leading to a reduction of spectral slopes at small wavenumbers. The same tendency is also found in other low-energy areas such as the eastern North Atlantic (not shown) where the k^{-2} slope of wavenumber spectra on long wavelengths has been interpreted as the impact of eddy generation by direct atmospheric forcing (Le Traon et al. 1990). The change of the spectra toward a plateau at long wavelengths when using more accurate WV corrections, however, supports the results from Fu (1983) and shows that wavenumber spectra at those wavelengths may not contain energy from ocean signals only. Therefore the interpretation in terms of ocean dynamics may be misleading as was pointed out by Stammer and Böning (1993). In contrast to the low-energy areas the SSH spectrum of the high-energy western North Atlantic (Fig. 5b) at midlatitudes (20°–40°N) is basically unchanged, because in this region the energy level of WV corrections at the low-wavenumber end of the spectrum is considerably lower than the SSH energy level.

To give a rough estimate of the influence of WV uncertainties on eddy scales derived from altimeter data, we calculated the linear integral scale $L_1 = [C(0)]^{-1} \int_0^{L_0} C(s)ds$ and the first zero-crossing L_0 of the autocovariance function C (for details see also Stammer and Böning 1992). Here s is the along-track distance. Both scales are listed in Table 2 for various 10° and 20° areas.

In the near-equatorial Atlantic (0°–20°N), the use of the SSM/I-We corrections results in a decrease of the along-track SSH correlation scale L_0 from 355 to 325 km (Table 2b). This is due to removing variability

at large scales associated with WV anomaly in the ITCZ (correlation scale L_0 about 400 km) (Fig. 6a, Table 2a). In the 20°–40°N latitude range the correlation scales for SSH and WV correction anomaly differ considerably (160 and 350 km, respectively) and thus WV corrections do not influence the SSH correlation scale in this high-energy western part of the basin (Fig. 6b, Table 2a). In the lower-energy eastern part (10°–40°W) the correlation scale between 20° and 40°N is larger and SSM/I-We corrections reduce large-scale variability as seen from the decrease of the L_0 scale from 255 to 210 km. Note that for the shorter 10° arcs in the northern part 30°–40°N, this large-scale effect almost vanishes. Likewise the integral correlation scale L_1, which is less selectively sensitive to large scales, shows WV correction influence in the near-equatorial region only. For FNOC WV corrections the energy is too small in both latitude ranges to have any significant effect on the wavenumber statistics.

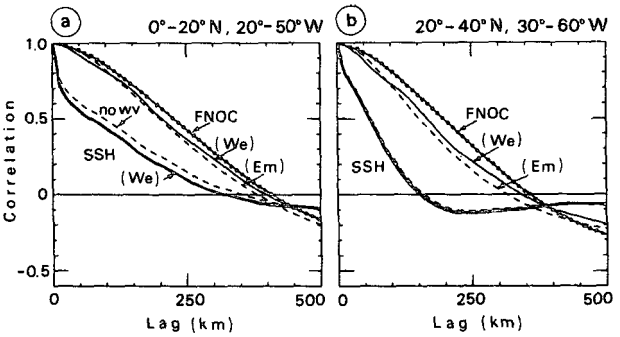

FIG. 6. Spatial autocorrelation function of WV correction anomaly and of SSH anomaly in (a) the western tropical and (b) the midlatitude North Atlantic.

6. Seasonal variation of SSH and velocity

The statistics of along-track SSH data and the wavenumber spectra indicated that WV variability close to the ITCZ has the strongest influence on the large-scale SSH variation. In this region the SSH variation is closely linked to the seasonal cycle of the equatorial circulation (DS). Previous Geosat altimeter studies in this region relied on FNOC WV corrections (Carton and Katz 1990; Arnault et al. 1990, 1992; DS92). To study the WV effect on the seasonal cycle of SSH and ocean currents in the 10°S–30°N latitude band, we use the 1-yr time series of monthly SSH anomaly maps resulting from interpolation of the along-track SSH anomalies by objective analysis.

The variability of the mapped SSH time series estimated without WV corrections is shown in Fig. 7a. Note that in contrast to the spatial and temporal variability of along-track SSH data in 2° × 2° cells (see Fig. 4a) the variability here contains only temporal variations at each grid point of the SSH time series smoothed by the space–time objective analysis procedure. A large fraction of the variance in the near-equatorial high-variability region is explained by annual harmonic fluctuations of the NECC (DS92). The variability of SSH without WV correction (Fig. 7a) is almost unchanged when FNOC WV corrections are applied: the maximum difference of rms variability is 0.4 cm. The influence of SSM/I-We WV corrections is shown by the rms of the difference signal between

TABLE 2. Eddy scales from autocorrelation functions estimated in regions extending over 20° and 10°.

(a) Scales of water vapor corrections

	L_1 (km)			L_0 (km)		
Area	FNOC	Wentz	Emery	FNOC	Wentz	Emery
20°–40°N, 30°–60°W	210	185	174	358	343	315
30°–40°N, 30°–60°W	164	143	143	294	269	265
0°–20°N, 20°–50°W	240	222	215	409	399	382

(b) Scales of SSH anomalies using different WV corrections

	L_1 (km)				L_0 (km)			
Area	No	FNOC	Wentz	Emery	No	FNOC	Wentz	Emery
20°–40°N, 30°–60°W	75	74	73	72	161	158	156	159
30°–40°N, 30°–60°W	73	72	71	—	139	138	136	—
20°–40°N, 10°–40°W	76	75	71	74	255	235	210	203
30°–40°N, 10°–40°W	59	58	56	57	142	141	137	137
0°–20°N, 20°–50°W	133	135	117	—	354	361	326	—
0°–10°N, 20°–50°W	85	86	75	76	233	235	212	213

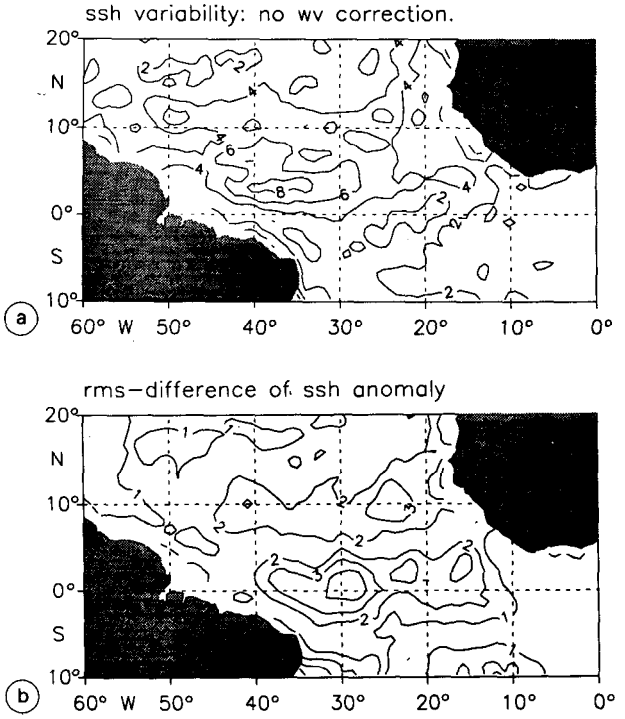

FIG. 7. SSH variability in the tropical Atlantic based on monthly objectively analyzed maps from August 1987 through July 1988. (a) SSH without WV corrections. (b) Root-mean-square of the difference between SSH with SSM/I-We correction and with no WV correction.

SSH without correction and SSH with SSM/I-We correction (Fig. 7b): maximum WV influence is observed near the equator and near 8°N, that is, at the southern and northern boundary of the high-SSH-variability region near 3°N. When SSM/I-Em corrections are used instead, the resulting spatial structure of SSH difference is similar, but maximum rms differences are slightly lower. The corresponding rms difference for FNOC corrections (not shown) is very small (<0.7 cm), except for a region close to the African continent, where it exceeds 1 cm.

The effect of WV corrections on the seasonal cycle in the western tropical Atlantic is most clearly shown by the meridional profiles of SSH anomaly (Fig. 8) averaged zonally between 30° and 40°W, that is, in the region of maximum SSH variability. The use of FNOC corrections (Fig. 8a) led to almost no change of SSH with respect to the uncorrected profiles (dashed lines). Amplitudes and seasonal variations of SSH are generally reduced when the SSH is corrected using the more realistic SSM/I-We WV data (Fig. 8b). Furthermore in most of the monthly profiles the SSH difference across the latitude range 3°–9°N of the eastward flowing NECC (DS92) is reduced.

Assuming geostrophic balance the seasonal variation of geostrophic surface velocity can be derived from the SSH slope. The monthly profiles of zonal velocity anomaly (Fig. 9) indicate that the strongest seasonal variations are centered in the 4°–6°N latitude band of the NECC core with maximum eastward velocity during September through January. The velocity anomaly south of 9°N is generally reduced by the SSM/I-We corrections. The zero crossing near 3°N, that is, the southern limit of the region in which velocity fluctuations are in phase with the NECC fluctuations, is shifted northward by almost 1° during the seasonal NECC velocity extrema.

The variation of inferred equatorial currents due to the WV uncertainty is summarized in Fig. 10, which shows the seasonal cycle of the zonal NECC core velocity (4°–6°N) based on the different WV datasets. Using the FNOC correction is almost equivalent to no WV correction: the rms difference is only 0.75 cm s^{-1}. The maximum difference between velocity based on FNOC and on SSM/I-We corrections is 14 cm s^{-1}; the rms difference is 8.1 cm s^{-1}. Note, that when SSM/I-Em instead of SSM/I-We corrections are used, the amplitude of the seasonal cycle of NECC velocity is diminished by less, indicating the impact of the uncertainty inherent in the WV retrieval from the same dataset. The maximum velocity difference resulting from the two WV corrections based on SSM/I data is 8 cm s^{-1} (in November 1987) and the rms difference is 3.8 cm s^{-1}.

The influence of WV corrections on the seasonal NECC velocity is summarized in Table 3: both the Emery and Wentz SSM/I WV corrections reduce the peak-to-peak amplitude of the seasonal signal. The rms variability of NECC velocity is reduced by 20% and 31% of the uncorrected value, respectively. In contrast, the FNOC WV corrections do not compensate for the seasonal WV variability in this region. This result demonstrates that the seasonal cycle of the tropical circulation derived from altimetry is significantly altered when using more reliable WV corrections.

7. Summary and conclusions

In this paper we provide a general indication of uncertainties in Geosat altimeter products due to WV corrections. Comparison between the FNOC and two SSM/I WV corrections provides insight into the sensitivity of altimetric products with respect to WV corrections and their associated errors.

Initial differences of 10–20 cm observed between FNOC and SSM/I WV corrections are due to the different WV estimation procedures and the different sampling and averaging space and timescales (section 2b). The filter effects of the collinear analysis (i.e., the linear operations of both 1-yr mean and quadratic polynomial subtraction) are shown to reduce much of the systematic differences: for all 3 WV datasets about half of the WV variability is filtered out on average over a 60°S–60°N track. The strongest WV influence

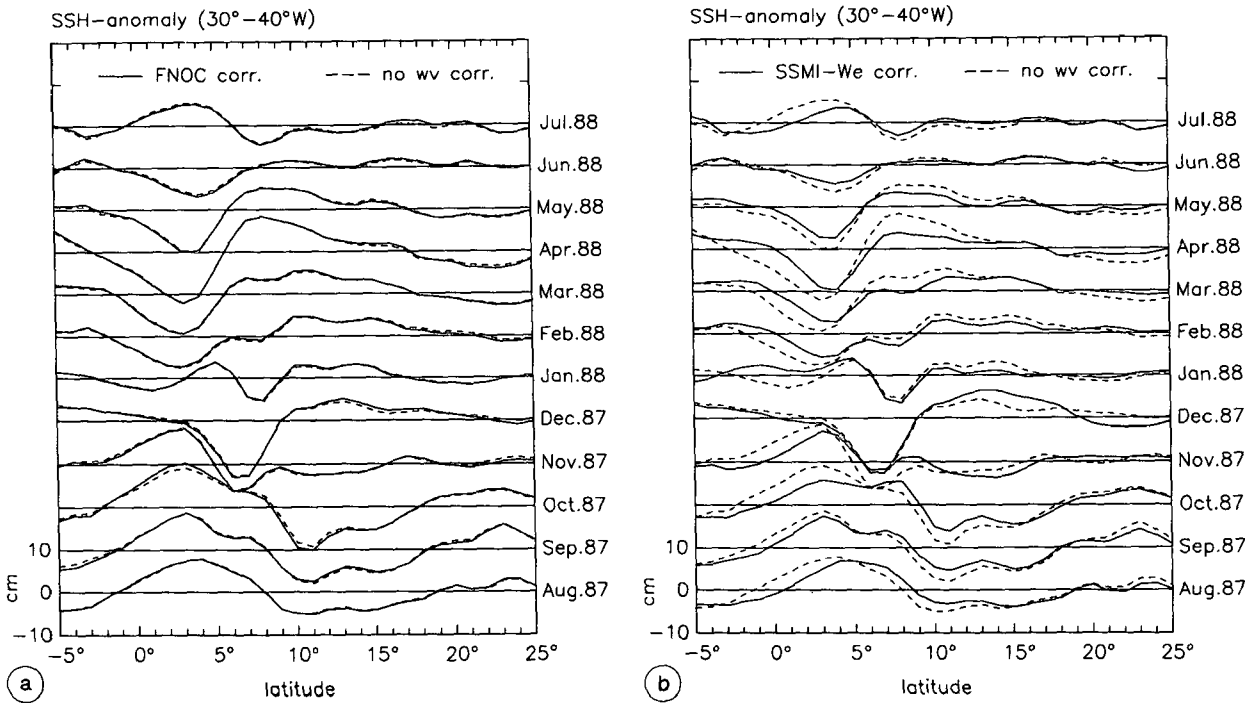

FIG. 8. Influence of (a) FNOC WV correction and (b) SSM/I-We WV correction on meridional profiles of SSH anomaly. The profiles based on monthly maps are zonally averaged over 30°–40°W. The offset is 10 cm.

on the final SSH anomaly is found in the western tropical Atlantic near 2° and 10°N at the turning latitudes of the seasonally migrating ITCZ, where SSM/I corrections reduce the along-track SSH variability by typically 1–1.5 cm. North of 20°N the influence of SSM/I corrections is small: the SSH variability changes by less than 0.5 cm. The FNOC corrections generally show very little effect on SSH anomaly: the variability changes by less than 0.3 cm with no increased level in the tropics.

No significant effect of SSM/I corrections on SSH wavenumber spectra and inferred eddy scales was found at midlatitudes (20°–40°N), where the correlation scales of WV and SSH are well separated. It should be kept in mind, however, that at mid- and high latitudes small-scale WV structures of high frequencies are not resolved in the interpolated SSM/I corrections (Phoebus and Hawkins 1990; Minster et al. 1992) and may still be present in the corrected SSH data. In the tropics (0°–20°N) the SSM/I WV energy level at wavelengths exceeding 600 km is high enough to reduce the uncorrected SSH variability and to change the spectral slope in this low-wavenumber range. The close match of correlation scales for WV (400 km) and for SSH (uncorrected: 355 km) leads to a shift of the SSH correlation scale to 325 km when applying SSM/I corrections. A similar tendency of the WV error to influence spectral characteristics on low wavenumbers is likewise found in other low-energy areas of the North Atlantic. Therefore one has to be careful while interpreting wavenumber spectra from altimeter data such as Geosat in terms of ocean dynamics as was pointed out recently by Stammer and Böning (1993).

For the tropical Pacific, Cheney et al. (1991) found improved agreement between tide-gauge data and Geosat low-frequency SSH time series when using SSM/I-We WV corrections. In the tropical Atlantic we observed maximum WV effects (caused by WV variability in the ITCZ) in the western 30°–40°W region: the rms difference of 2–3 cm between uncorrected and SSM/I-We–corrected SSH time series, based on objectively analyzed monthly maps, characterizes the maximum WV effect on seasonal timescales. The corresponding variability of the seasonal cycle of geostrophic zonal velocity in the NECC core is reduced by 20% when changing from FNOC corrections (or no WV corrections) to SSM/I-Em corrections and by 31% for SSM/I-We corrections.

Differences between WV corrections, which are related to the lack of simultaneous WV measurements, will not effect ongoing and future missions equipped with microwave radiometers on board the satellite. However, differences due to different WV retrieval algorithms will remain a potential source of uncertainty for *ERS-1* and Topex–Poseidon altimetry with simultaneous microwave radiometer measurements. Thus our results on the sensitivity of altimetric SSH anomaly to WV correction differences

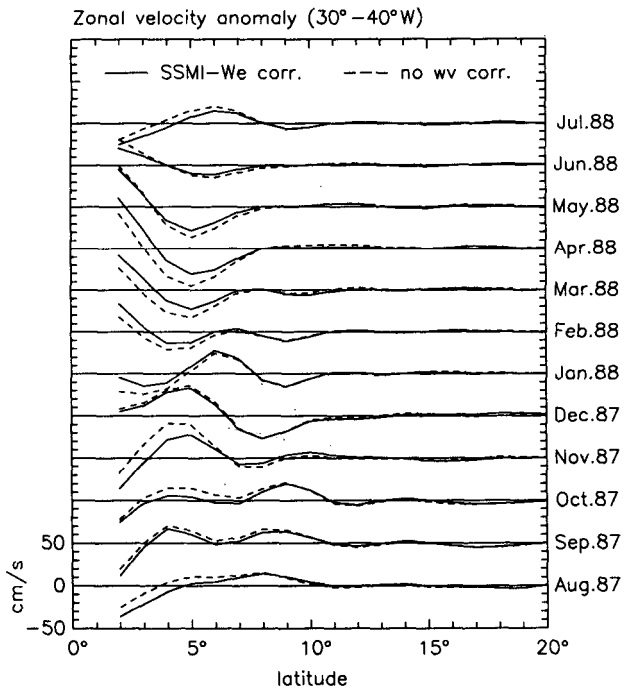

FIG. 9. Meridional profiles of zonal geostrophic velocity anomaly, zonally averaged over 30°–40°W. The monthly profiles for SSM/I-We correction (solid) and no WV correction (dashed) are displayed with an offset of 50 cm s^{-1}.

(or correction errors) clearly indicate, that for high-quality altimeter products from this new altimeter generation, a reliable WV retrieval algorithm is particularly important for the atmospheric conditions in the tropics.

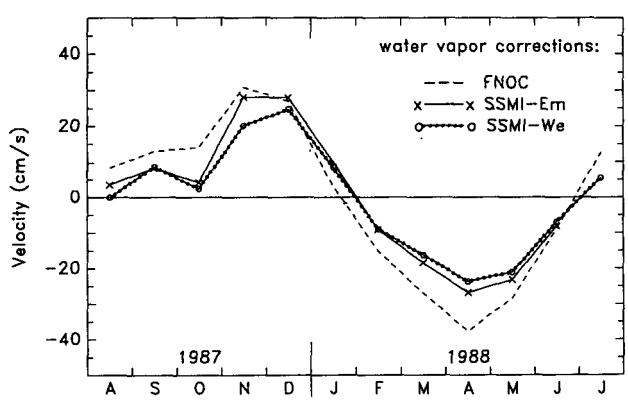

FIG. 10. The influence of WV corrections on the seasonal cycle of zonal geostrophic velocity anomaly in the NECC core region 4°–6°N, 30°–40°W.

TABLE 3. Influence of WV corrections on seasonal variations of zonal velocity in the NECC core region 4°–6°N, 30°–40°W.

WV correction	Peak to peak (cm s^{-1})	σ (cm s^{-1})	$\Delta(\sigma)/\sigma$ (no correction)
No WV correction	69.2	21.4	—
FNOC	68.6	21.5	0.5%
SSM/I-Em	54.8	17.1	−20.1%
SSM/I-We	48.4	14.7	−31.3%

Acknowledgments. The authors are grateful to W. Emery, who kindly provided his global SSM/I water vapor dataset. The support of this study by the DFG (SFB 133) (ND) and the BMFT (Grant No. 07 KFT 460) (DS) is gratefully acknowledged.

REFERENCES

Arnault, S., Y. Ménard, and J. Merle, 1990: Observing the tropical Atlantic Ocean in 1986–1987 from altimetry. *J. Geophys. Res.*, **95**(C10), 17 921–17 945.

——, A. Morlière, and J. Merle, 1992: Low frequency variability of the tropical Atlantic surface topography: Altimetry and model comparison. *J. Geophys. Res.*, **97**(C9), 14 259–14 288.

Carton, J. A., and E. J. Katz, 1990: Estimates of the zonal slope and seasonal transport of the Atlantic North Equatorial Countercurrent. *J. Geophys. Res.*, **95**(C3), 3091–3100.

Chelton, D. B., 1988: WOCE/NASA Altimeter Algorithm Workshop. U.S. WOCE Tech. Report No. 2, U.S. Planning Office for WOCE, 70 pp. [Available from Texas A & M University, College Station, TX 77843.]

Cheney, R. E., B. C. Douglas, R. W. Agreen, L. Miller, D. L. Porter, and N. S. Doyle, 1987: Geosat altimeter geophysical data record user handbook. NOAA Tech. Memo. NOS NGS-46, 32 pp. [Available from National Geodetic Survey, NOAA, Rockville, MD 20852.]

——, W. J. Emery, B. J. Haines, and F. Wentz, 1991: Recent improvements in Geosat altimeter data. *EOS, Trans. AGU*, **72**, 577–580.

DeMey, P., and Y. Ménard, 1989: Synoptic analysis and dynamical adjustment of GEOS3 and Seasat altimeter fields in the northwest Atlantic. *J. Geophys. Res.*, **94**(C5), 6221–6230.

Didden, N., and F. Schott, 1992: Seasonal variations in the western tropical Atlantic: Surface circulation from Geosat altimetry and WOCE model results. *J. Geophys. Res.*, **97**(C3), 3529–3541.

——, and ——, 1993: Eddies in the North Brazil Current retroflection region observed by Geosat altimetry. *J. Geophys. Res.*, **98**, 20 121–20 131.

Emery, W. J., G. H. Born, D. G. Baldwin, and C. L. Norris, 1990: Satellite-derived water vapor corrections for Geosat altimetry. *J. Geophys. Res.*, **95**(C3), 2953–2964.

Fu, L.-L., 1983: On the wave number spectrum of oceanic mesoscale variability observed by the Seasat altimeter. *J. Geophys. Res.*, **88**, 4331–4341.

——, and V. Zlotnicki, 1989: Observing ocean mesoscale eddies from Geosat altimetry: Preliminary results. *Geophys. Res. Lett.*, **16**, 457–460.

Gordon, A. L., and W. F. Haxby, 1990: Agulhas eddies invade the South Atlantic: Evidence from Geosat altimeter and shipboard CTD survey. *J. Geophys. Res.*, **95**(C3), 3117–3125.

Holland, W. R., V. Zlotnicki, and L.-L. Fu, 1992: Modelled time dependent flow in the Agulhas retroflection region as deduced from altimeter data assimilation. *South African J. Mar. Sci.*, **10**, 407–427.

Jourdan, D., C. Brossier, A. Braun, and J.-F. Minster, 1990: Influence of wet tropospheric correction on mesoscale dynamic topography as derived from satellite altimetry. *J. Geophys. Res.*, **95**(C10), 17 993–18 004.

LeTraon, P. Y., M. C. Rouquet, and C. Boissier, 1990: Spatial scales of mesoscale variability in the North Atlantic as deduced from Geosat data. *J. Geophys. Res.*, **95**(C11), 20 267–20 285.

Minster, J.-F., D. Jourdan, E. Normant, C. Brossier, and M. C. Gennero, 1992: An improved special sensor microwave imager water vapor correction for Geosat altimeter data. *J. Geophys. Res.*, **97**(C11), 17 859–17 872.

Moore, A., 1991: Data assimilation in a quasigeostrophic open-ocean model of the Gulf Stream region using the adjoint method. *J. Phys. Oceanogr.*, **21**, 398–427.

Phoebus, P. A., and J. D. Hawkins, 1990: The impact of the wet tropospheric correction on the interpretation of altimeter-derived ocean topography in the northeast Pacific. *J. Geophys. Res.*, **95**(C3), 2939–2952.

Saastamoinen, J., 1972: Atmospheric correction for the troposphere and stratosphere in radio ranging of satellites. *Geophys. Monogr.*, No. 15, Amer. Geophys. Union, 247–251.

Stammer, D., and C. W. Böning, 1992: Mesoscale variability in the Atlantic Ocean from Geosat altimetry and WOCE high-resolution numerical modeling. *J. Phys. Oceanogr.*, **22**, 732–752.

——, and ——, 1993: Reply. *J. Phys. Oceanogr.*, **23**, 2733–2735.

——, H.-H. Hinrichsen, and R. H. Käse, 1991: Can meddies be detected by satellite altimetry? *J. Geophys. Res.*, **96**(C4), 7005–7014.

Tai, C.-K., 1989: Accuracy assessment of widely used orbit error approximations in satellite altimetry. *J. Atmos. Oceanic Technol.*, **6**, 147–150.

Tapley, B. D., J. B. Lundberg, and G. H. Born, 1982: The Seasat altimeter wet tropospheric range correction. *J. Geophys. Res.*, **87**, 3213–3220.

Wentz, F. J., 1983: A model function for ocean microwave brightness temperatures. *J. Geophys. Res.*, **88**(C3), 1892–1908.

——, 1990: User's manual collocated Geosat-SSM/I tape. Tech. Rep. 100190. [Available from Remote Sensing System, 1101 College Ave., Santa Rosa, CA 95404.]

White, W. B., C.-K. Tai, and W. R. Holland, 1990: Continuous assimilation of simulated Geosat altimetric sea level into an eddy-resolving numerical ocean model. Part 1: Sea level differences. *J. Geophys. Res.*, **95**(C3), 3219–3234.

Willebrand, J., R. H. Käse, D. Stammer, H.-H. Hinrichsen, and W. Krauss, 1990: Verification of Geosat sea surface topography in the Gulf Stream extension with surface drifting buoys and hydrographic measurements. *J. Geophys. Res.*, **95**(C3), 3007–3014.

Zimbelman, D. F., and A. J. Busalacchi, 1990: The wet tropospheric range correction: Product intercomparisons and the simulated effect for the tropical pacific altimeter retrievals. *J. Geophys. Res.*, **95**(C3), 2899–2922.